Proceedings of the 24th ASM Heat Treating Society Conference, September 17-19, 2007
COBO Center, Detroit, Michigan, USA.

Effective Design of Heat Treat Processes Using Computer Simulations

Zhichao Li, Andrew M. Freborg and B. Lynn Ferguson
Deformation Control Technology, Inc.
7261 Engle Road, Suite 105
Cleveland, OH 44130

Abstract

With over two decades of development, computer simulation of heat treat processes has improved significantly. Wider capabilities and improved accuracy, as well as growing material databases and robust support systems in commercial softwares are all evidence of this improvement. As a result, the heat treatment industry has reached a critical technical juncture in its vision towards improved quality and costs. Now is the right time to begin more aggressive use of simulation in heat treatment engineering, especially in such areas as process trouble shooting and process/part design. To demonstrate the potentials, this paper reports on the use of computer simulation to optimize the water spray quenching process of an induction hardening of a spur gear. Compared to traditional quench hardening practices, induction hardening of steel parts is increasingly being used for the following reasons: i) the process is more consistent on a part-to-part basis, making it easier for quality control; ii) because water is the typical cooling agent, it is environmentally friendly; iii) higher and deeper surface compressive residual stress can be achieved in comparison to oil quenching and thus fatigue life is improved.

In this paper, the finite element based software DANTE® was used to simulate and design the water spray quenching step of an induction hardening processes for a thin walled spur gear made of carburized AISI 5120 or AISI 5130 steels. The heat generated by the induced eddy currents was used as input to drive the heating model. An optimization method based on sensitivity analysis was combined with heat treatment simulations to improve the spray quenching process after induction heating. The objective function was defined to minimize the distortion of the gear tooth while satisfying the residual stress and microstructure requirements, and a maximum bore surface temperature constraint. The residual stress state predicted after induction hardening was then mapped into a 3D whole gear model to predict the internal stress change due to a tooth bending fatigue load. The significance of considering residual stresses from heat treatment in designing bending fatigue test is addressed.

Key words: Induction Hardening, Distortion, Finite Element Method, Phase Transformation, Optimization, Residual stress

Introduction

Induction hardening has achieved more wide acceptance recently due to some advantages over traditional hardening processes. During induction hardening, heat is generated in the part surface by induced eddy currents. The heat density distribution through the surface is directly related to the distance between the inductor and part surface, and the frequency of the inductors. Lower frequency tends to heat the the part deeper (over a longer time) because the eddy current gradient in the part surface is relatively low. In contrast, a higher induction frequency heats a more shallow layer at the part surface over a shorter time. The temperature distribution in the part is a combined result of thermal conduction and induction heating.

In many induction hardening processes, both low/medium frequency and high frequency settings are used together to reach the desired temperature field. Simultaneous dual fequency (SDF) induction heating is another process used in industry.[1] Different from standard induction heating, SDF induction heating applies two frequncies in the part simultaneously. By using different percentages of the two frequencies, SDF induction heating provides greater flexibility in controlling temperature distribution within a part of complicated shape such as a gear.

Induction hardening is a transient thermal process. During induction hardening of steel components, the temperature gradient and phase transformations simultaneously contribute to the evolution of internal stresses and distortion. Recent enhancements in heat treatment simulation software make it much easier to understand the material response during the heat treatment process, such as how the internal stresses and deformation are generated. DANTE is a commercially available heat treatment software based on finite element method.[2] DANTE is not designed to model the physics of induction heating process; however, DANTE can be used to simulate the temperature field during induction heating by using Joule heating based on the eddy current distribnution in the part, i.e. i^2r heating.

Optimization methods have been used in many manufacturing fields to improve process design, reduce product weight, and improve profit. For example, optimization has been used for obtaing the heat transfer coefficients during oil quenching of a helical spur gear from thermocouple experiments.[3] Another example is use of the Response Surface method in optimizing a gas quenching process.[4, 5] Included in both of these examples of optimization methods for determining process parameters were the phase transformation and latent heat effects. The ability to include these types of physical

phenomena in optimization analysis makes it a robust, accurate, and uselful calculation method for the heat treatment industry.

For this study, optimization based on Sensitivity Analysis was applied to the cooling process after induction heating. The sensitivity information is calculated using the finite difference method, with the sensitivity information providing a direction for finding the the optimized design. The main drawback of the method is that the searching process for the optimum design may be stopped by a local minimum point. In most cases, a global minimum point in the design range is preferred.

Finite Element Simulation of Induction Hardening Process

Finite element simulations were used to model the induction hardening process. The material database in DANTE covers most low and medium carbon steels. The data required for heat treat simulation includes thermal properties, phase transformation kinetics, and mechanical properties of each individual phase over the range of temperatures and heating/cooling rates for the process. The accuracy of the model is of course directly related to the accuracy of the material data. Data development efforts include dilatometry testing for kinetics, tension or compression tests at different temperatures for mechanical properties, as well as validation of simulation results with experimental studies.[6, 7] For this paper, two steel grade options for the gear were evaluated: AISI 5120 and AISI 5130. The heat treatment process for this gear includes vacuum carburization, followed by relatively slow cooling to achieve a normalized microstructure, and then induction hardening.

Finite Element Model

The geometry of the spur gear is shown in Figure 1. The gear has a total of 60 outer teeth, with a bore diameter of 164 mm (6.45 in.), a tip diameter of 195.59 mm (7.70 in.), and a height of 60 mm (2.36 in.). The tooth height (radial distance from the gear root to the gear tip) is about 6.1 mm (0.24 in.), and the wall thickness (distance from the bore surface to the gear root) is about 10 mm (0.39 in.).

A simplified two dimensional plane strain model of a single gear tooth was used for the heat treatment simulations and design optimization. The finite element mesh for the model is shown in Figure 2, and it consists of 884 nodes, and 824 4-node linear elements. As shown in Figure 2, the elements at the part surface are more finely spaced to accurately capture the steep thermal and carbon gradients during quenching. A cyclic symmetry boundary condition was used during the analysis. By using cyclic symmetry, the 60 teeth are assumed to align along the circumferential direction uniformly, meaning that the gear will remain circular and will not become oval for this analysis. The 3 points P1, P2, and P3 in Figure 2 are referenced later in defining the optimization process.

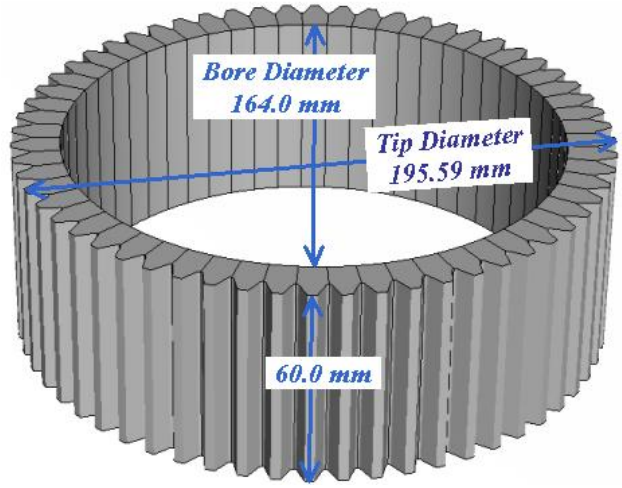

Figure 1: Spur gear geometry with 60 teeth.

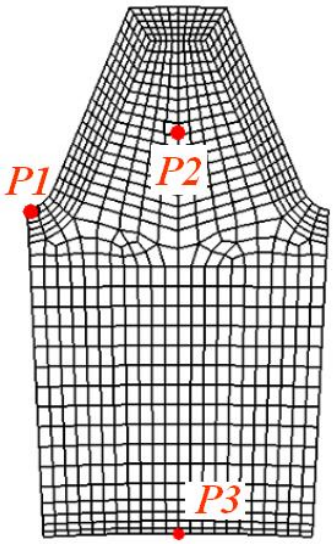

Figure 2: 2D Plane Strain Finite Element Mesh.

Modeling of Vacuum Carburization Process

As mentioned, two steels were examined in these models, AISI 5120 and AISI 5130. Both of these steels require carburization in order to meet surface hardness requirements. For these models, vacuum carburization of the gear was simulated, using a furnace temperature of 950ºC (1742ºF) and acetylene gas as the carbon source. The partial pressure of the acetylene was 1.5 torr during the boost steps, and the vacuum carburization schedule included two boost/diffuse steps, as listed in Table 1.

Table 1: Vacuum carburization schedule.

	Step 1	Step 2
Boost (sec)	225.7	411.4
Diffuse (sec)	1298.5	2041.8

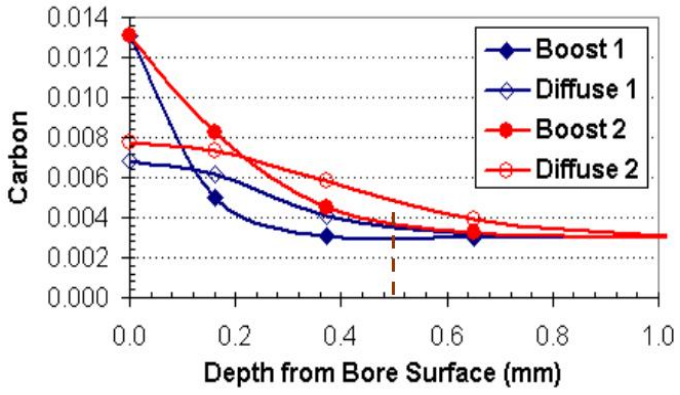

(a)

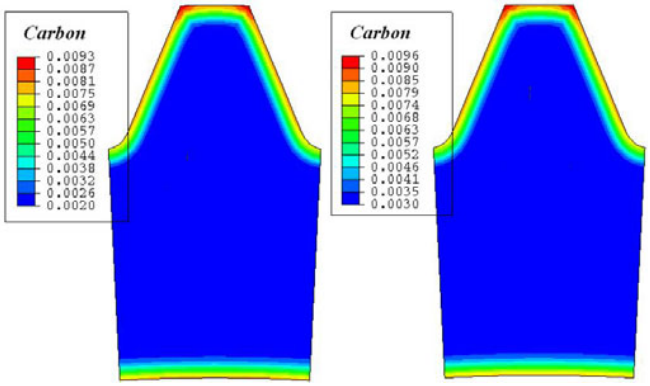

(b) (c)

Figure 3: Carbon Distributions (a) in terms of depth from bore surface at different boost/diffuse steps for 5130 steel; (b) carbon weight fraction contour plot for AISI 5120 gear; and (c) carbon weight fraction contour plot for AISI 5130 gear.

During vacuum carburization, the acetylene gas dissociates on the surface of the hot part. The exposed surface of the austenitized gear reaches carbon equilibrium in a short time (less than 5 seconds). Because of the excellent penetration of acetylene, the difference in time for the gear tip and gear root to reach the carbon equilibrium is negligible. The carbon equilibrium of AISI 51XX steel at 950º C is about 1.35%. Using AISI 5130 as an example, the predicted carbon distributions in the bore surface at different vacuum carburization steps are shown in Figure 3(a), where the X-axis is the depth from the bore surface, and the Y-axis is the carbon content. After the first boost step of 225.7 seconds, the carbon distribution is shown by the line with solid diamond marks. During diffusion, there is no acetylene flowing to the part surface and the carbon stored in the surface layer during the boost step diffuses toward the part interior. After the first diffusion period of 1298 seconds, the surface carbon decreases to about 0.7%. The second boost step raises the surface carbon to its equilibrium again in a short time. After the second diffusion step, the carbon distribution in the bore surface is shown as the line with hollow round marks (cf. Figure 3(a)). The carbon content on the bore surface is about 0.8%, and the case depth is about 0.5 mm.

Figures 3(b) and (c) show the carbon contour plots at the end of vacuum carburization for the two steel grades, respectively. The differences in case depth and carbon distribution in the case are due to the difference in base carbon level. In addition, the geometry effect on the carbon distribution is significant. The carbon content on the tip surface is over 0.9% in both steels, as shown in the carbon contour plots, and the carbon content on the tooth flanks is less than 0.8%; this difference is more than 0.1%. High carbon content on the gear tip location leads to a higher volume fraction of retained austenite after spray quenching, which may cause problems such as low hardness and dimensional instability due to the potential for further phase transformation. To solve this problem, round corners instead of sharp corners at the tooth tip are preferred. For gears with special requirements, the tooth tip surface can be copper plated to avoid excessive carbon penetration, as is often the case in aerospace gears, or a deep freeze step to reduce the retained austenite fraction may be performed after spray quenching.

Modeling of the Induction Heating Process

The induction heating schedule for this specific gear includes both low frequency heating and high frequency heating. The low frequency heating time period is 3.0 seconds, and the temperature and austenite distributions at the end of the 3.0 seconds heating are shown in Figure 4(a). The temperature of the gear root at this time is predicted to be 1000º C, and the gear root is fully austenitized. The temperature at the gear tip is about 600º C, which is below is the austenite formation temperature. It is important to form austenite in the root during the low frequency heating, because the subsequent high frequency heating focuses on the tip location of the gear.

Following the low frequency heating, the gear is held for 0.5 seconds before high frequency heating is applied. Heat in the gear root diffuses away during this stage. At the end of the hold, the temperature distribution is as shown in Figure 4(b). Tooth temperature is between 600 and 700º C, which is below the austenite forming temperature, and there is no significant austenite formed due to thermal conduction during this stage. After the 0.5 seconds hold, the gear is heated for 0.5 seconds under high frequency. The heating focuses mainly on the tooth tip, and decreases toward the gear root location. The temperature and austenite distributions after the high frequency heating are shown in Figure 4(c). The tip of the gear has the highest temperature, around 1070ºC, after the high frequency heating. At this time most of the gear tooth is

austenitized, as shown in Figure 4(c).

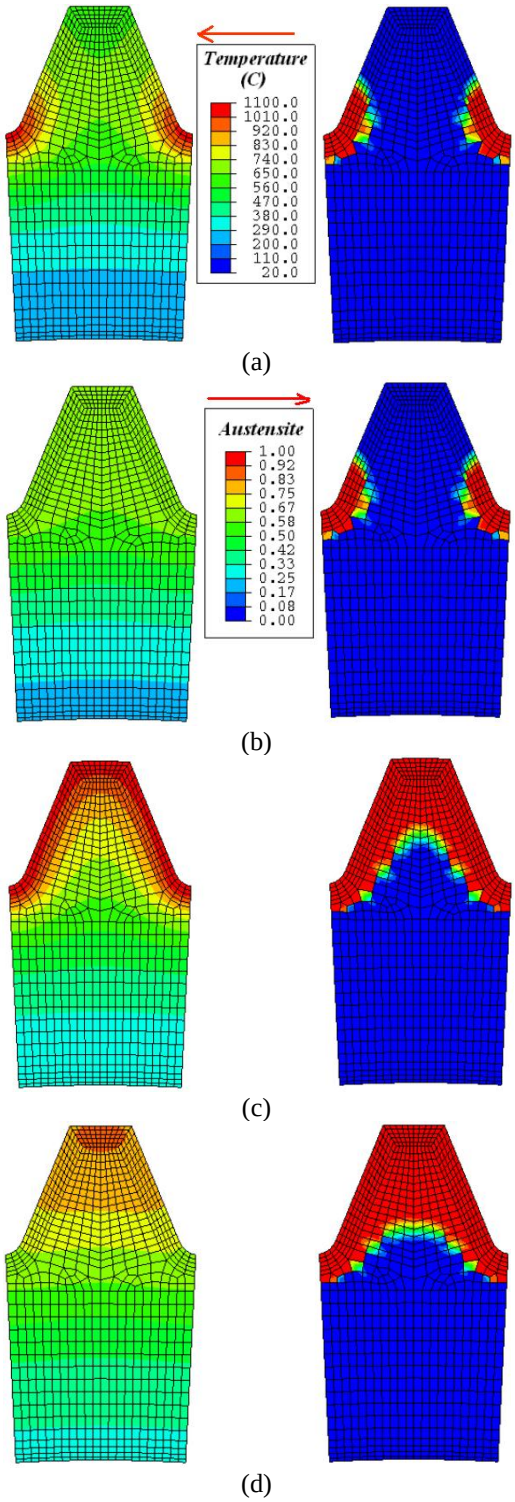

Figure 4: Temperature and austenite distribution at different induction heating stages (a) the end of 3.0 seconds of low frequency heating; (b) the end of a 0.5 second dwell; (c) the end of 0.5 seconds of high frequency heating; and (d) the end of a 0.5 second delay before spray quenching.

After the high frequency heating and before the water spray quenching, a controlled delay time may be used to adjust the thermal gradient in the gear. This delay affects the distortion and residual stress distributions of the final gear. In a later section of this paper, the delay time is used as one of the design variables to optimize the quenching process. For the example presented here, a 0.5 second delay is simulated to analyze its effect on temperature and austenite content. Due to thermal conduction, the temperature in the core of the gear tooth increases, and more austenite is formed in the core, as shown in Figure 4(d). Here the surface temperature of the bore has reached about 350º C.

Optimization of the Spray Quenching Process

Both heating and spray quenching have a significant effect on induction hardening response. In this study, the induction heating process was fixed and only a limited number of spray quench process variables were considered as design variables for optimization. Due to their significant effect on the hardening results, the three design variables selected were:
1) the heat transfer coefficient applied on the gear tooth surface; 2) the heat transfer coefficient applied on the bore surface; and 3) the delay time before spray quenching.

Distortion from heat treatment is a big concern within the industry. Part distortion often requires additional machining, and thus increases overall manufacturing cost. Distortion can also cause increased operating noise and reduced fatigue life in gears. Minimizing heat treat distortion is therefore an important manufacturing goal. For these gear simulations, the microstructure of the gear before heat treatment was assumed to be a mixture of ferrite and pearlite. After induction hardening, the gear tooth has transformed to martensite. Because martensite has a lower density compared to the ferrite/pearlite structure, the gear tip is expected to grow after induction hardening. A rough calculation using FEA shows that the expected radial expansion of the gear tip due to the phase change from ferrite/pearlite to martensite is about 25 µm. This projected gear radial expansion can be used during design of the gear geometry to adjust the green shape to minimize subsequent machining required due to radial growth. In this analysis, distortion was defined as the difference in the radial displacement of the gear tip from the expected growth of 25 µm. The objective function of the optimization model was set-up to minimize the gear distortion at the end of induction hardening as shown by equation (1).

The residual stress distribution in the gear root and adjacent areas after heat treatment has a direct relation to the bending fatigue life of the gear. Generally, greater surface compressive stress leads to improved fatigue life. The gear models presented in this paper are vacuum carburized, so compressive surfaces stresses are expected. The first constraint of this optimization model requires a minimum of 500 MPa

compressive residual stress in the near root location, as shown by point P1 in Figure 2. The first constraint in normalized format is shown in equation (2).

The microstructure in the core of the gear tooth is also an important factor in characterizing the induction hardening process. The induction heating simulation showed that location P2 in Figure 2 is austenitized. In this optimization analysis, a minimum of 95% martensite is required at the location P2 after hardening, and this requirement is used as the second constraint (cf. equation (3)).

The third constraint applied to the optimization model is that the maximum temperature on the bore surface before spray quenching should not exceed 370ºC. This constraint is a function of the specific inductor and spray system fixture design, and is shown in equation (4).

The optimization model is thus described by the following equations:

Objective:

$$\text{To minimize: } Distortion = |U_R - 25.0| \quad (1)$$

where U_R is the radial displacement of the gear tip in microns.

Constraints:

$$C1 = S_{P1} / 500.0 + 1.0 \le 0.0 \quad (2)$$

$$C2 = 0.95 - VF_m \le 0.0 \quad (3)$$

$$C3 = T_{P3} / 370.0 - 1.0 \le 0.0 \quad (4)$$

where S_{P1} is the residual stress in the circumferential direction at point P1; VF_m is the volume fraction of martensite at point P2; and T_{P3} is the temperature at the bore surface before spray quenching.

The flow chart in Figure 5 summarizes how the optimization procedure is implemented. First, the optimization model should be defined for the specific induction hardening process, including the objective function, constraints, and the design variables. The objective function and constraints should also be sensitive to the design variables. The lower and upper bounds of the design variables then need to be defined. The range of the design variables should cover the optimum point, and, most important, be industrially practical. For this optimization case study, the ranges of the design variables are listed in Table 2. Note, the ability to spray quench both the OD and ID of the ring gear was assumed, and some facilities may not have this capability. The heat transfer coefficients are assumed to be constants based on the assumption that the boiling and vapor blanket at the early quenching stage are eliminated by high quench water velocity. A delay time of 0.0 seconds means that there is no time delay and the water spray starts immediately after the high frequency induction heating. Previous modeling results show that the bore surface temperature will exceed 400º C with delay times exceeding 2.0 seconds. Because the heating schedule is fixed, the bore surface temperature before quenching is controlled principally by the delay time. The delay time for a satisfactory design should therefore be less than 2.0 seconds.

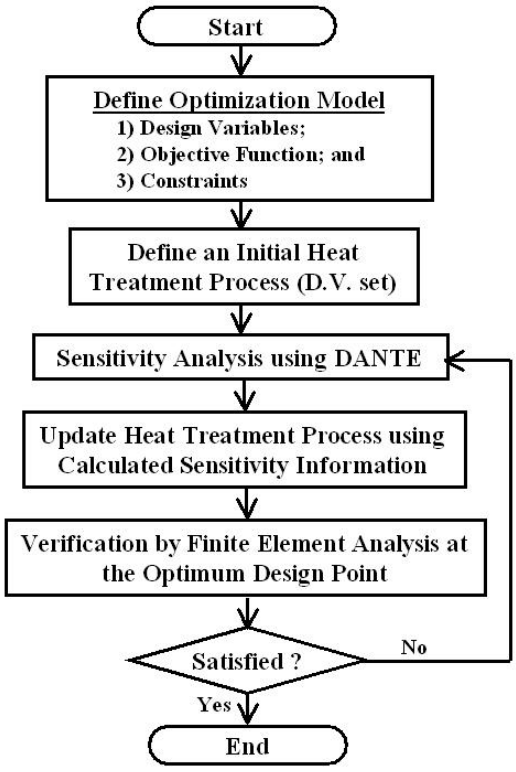

Figure 5: Flow chart of optimization procedure.

Table2: Lower and upper bounds of design variables.

	DV 1 (W/mm2C) (H on tooth surface)	DV 2 (W/mm2C) (H on bore surface)	DV 3 (second) (Delay time)
Lower Bound	0.005	0.005	0.0
Upper Bound	0.02	0.02	2.0

The design optimization procedure starts from an initial guess point (spray quenching design). Using finite differences, the sensitivities of the objective function and constraints in terms of all the three design variables are calculated by the DANTE simulation for this initial design. The sensitivity information then provides a direction for an intermediate optimum design, and the three spray quenching process variables are updated accordingly. Because heat treatment is a highly nonlinear process, the updated design requires additional simulations to evaluate distortion, residual stress, temperature, and phase distributions. The procedure iterates until it reaches a converged and satisfactory solution.

As shown in Figure 6, for iteration no. 1 (initial guess point) the heat transfer coefficients on both the gear tooth surface and the bore surface are 0.01 (*W/mm^{2}C)*; and the delay time is 1.0 seconds. After finite element simulation using this initial guess point, three more simulations were run with a small change in the three design variables, so that the sensitivity information for all the design variables could be calculated. Figure 7 shows that simulation results after induction hardening revealed no significant differences among the first four iterations.

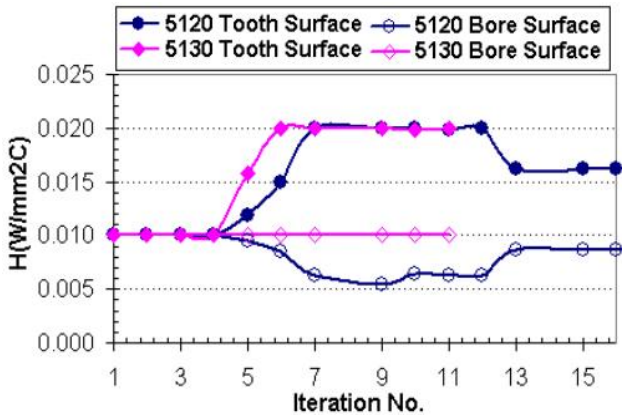

(a)

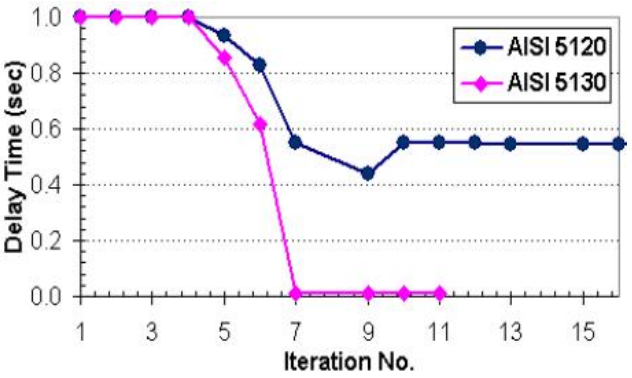

(b)

Figure 6: Evolutions of design variables: (a) heat transfer coefficients; and (b) delay time before spray quench with optimization iterations.

Once the sensitivity information is available, an improved design can be determined using the optimization algorithm. Using the gear made of AISI 5120 as an example, the intermediate optimum designs (iteration No. 5 and 6) tend to increase the heat transfer coefficient value on the bore surface, while reducing the heat transfer coefficient on the tooth surface (cf. Figure 6(a)). In Figure 7(a), the red horizontal line represents the expected radial expansion of the gear tip surface due to phase transformation; This expansion is ~25μm as discussed previously. Also as mentioned before, distortion is defined as the difference between the radial displacement and the expected radial expansion. For both iterations 5 and 6, the distortion tends to decrease. The residual stress and microstructure constraints are also satisfied for both iterations. However the bore surface temperature is above 375º C, which violates the third constraint. From iterations 7 to 12, the intermediate design tends to converge. The heat transfer coefficient on the tooth surface is about 0.006 W/(mm^{2}C). The heat transfer coefficient on the bore surface is 0.02 W/(mm^{2}C), which is the upper bound of this design variable. The resulting radial expansion is about 17 μm, which leads to bout 8 μm distortion through comparison to the expected radial expansion. As mentioned before, the bore surface temperature before spray quenching is mainly controlled by the delay time, and it is not sensitive to the other two design variables. The delay time now converges at about 0.54 seconds. The corresponding bore surface temperature is now 370º C, which satisfies the temperature constraint as shown in Figure 6(b). Comparing to AISI 5130, the AISI 5120 has lower hardenability. With a lower heat transfer coefficient applied on the gear tooth surface, the microstructure constraint is not satisfied from iterations 7 to 12 for the 5120 gear (cf. Figure 7(c)). The residual stress requirement is also not satisfied for this design iteration range.

From these intermediate iterations, a conclusion can be made that the heat transfer coefficients are important to the residual stress in the gear root. A higher heat transfer coefficient on the gear tooth surface and a lower heat transfer coefficient on the bore surface tend to generate higher compressive residual stress in the gear root. Because the constraints on the residual stress and microstructure are not satisfied from iterations 7 to 12, more optimization iterations are required. As shown by Figure 6(a), the heat transfer coefficient on the bore surface tends to decrease, while the heat transfer coefficient on the tooth surface tends to increase in iteration 13. The residual stress requirement is now satisfied with the new design point. The heat transfer coefficients on the tooth surface and bore surface are 0.008 and 0.016 (*W/mm^{2}C)*, respectively. The heat transfer coefficients applied on the gear surface affect not only the residual stress in the gear root, but also the radial displacement, as shown by the iterations from 13 to 16 in Figure 7(a). The distortion at the final optimum design point is less than 1.0 μm with all the constraints satisfied. Among the three constrains, the residual stress and the bore surface temperature constraints remain active.

For the gear made of AISI 5130, the microstructure constraint is easily satisfied because of the material's high hardenability. An optimum design is obtained after only 11 iterations, and the distortion of the optimum design is less than 1.0 μm (cf. Figure 7(a)). All the constraints are satisfied at this design point, with only the residual stress constraint active.

For the optimum design point of the 5130 gear, contour plots of radial displacement, circumferential residual stress, and martensite distribution are shown in Figure 8. Comparison of the martensite and radial displacement plots shows that the phase transformation has significant effect on the gear tip displacement. Figure 8(a) shows the variation of the radial

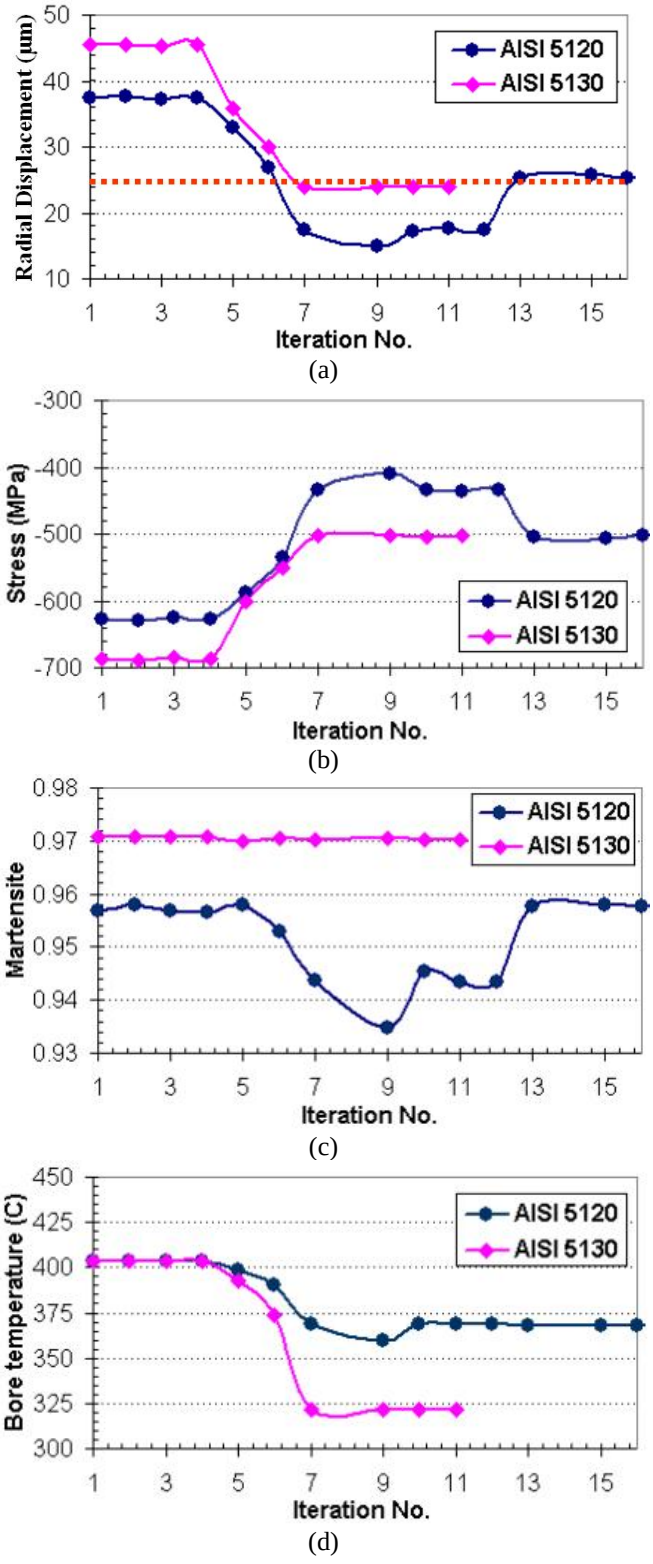

Figure 7: Evolutions of (a) distortion; (b) residual stress; (c) martensite volume fraction; and (d) bore temperature with optimization iterations.

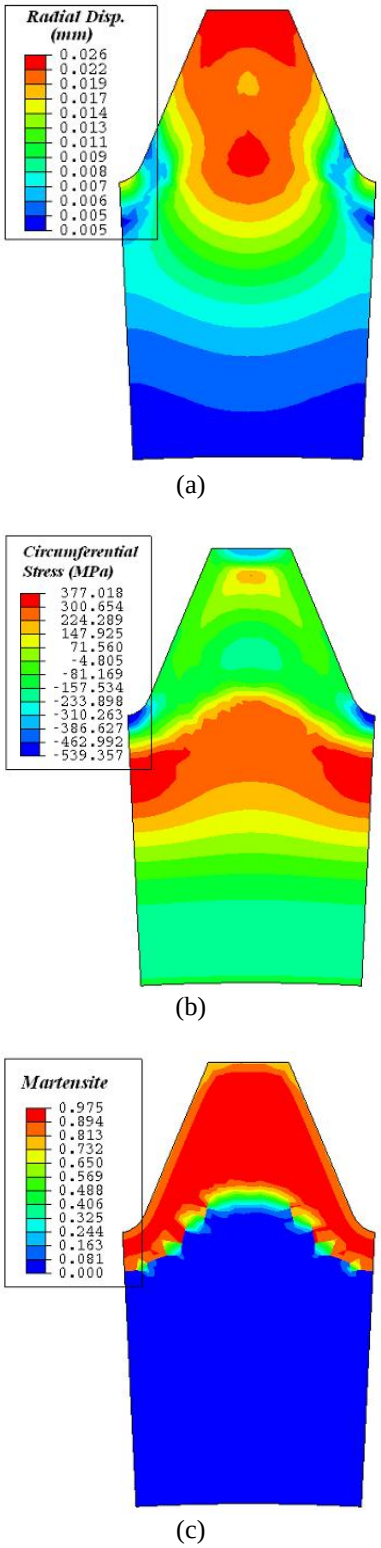

Figure 8: Optimized result for gear made of AISI 5130: (a) Radial distortion; (b) Circumferential stress; and (c) Martensite distribution

displacement along the gear tooth surface. Distortion of the gear surface profile can also be used as an objective function to optimize the induction hardening process. Figure 8(b) shows tensile stresses in the circumferential direction under the gear tooth to balance the compressive residual stress in the gear tooth root. The tensile stress region in Figure 8(b) was not austenitized.

The residual stress distribution in the gear root significantly affects the gear's bending fatigue life [8]. In general, compressive residual stress in the gear root improves bending fatigue life. However, most stress calculations used for gear bending fatigue characterization do not include the residual stress effect from heat treatment processes. This is mainly because the residual stress pattern after heat treatment or from processes such as shot peeing and burnishing are unknown for most parts. It is now possible to predict the material response during heat treatment of a part so that the residual stress state can be incorporated into gear tooth bending stress models as the starting condition.

To demonstrate this important ability, a 3D single tooth model was generated to predict the residual stress profile after induction hardening. The induction hardening process simulated was the optimized process for the gear made of AISI 5130. The residual stress state of the 3D single tooth model was mapped to a whole gear model to predict the stress change under a tooth bending load. A mechanical model was then executed in which the bending load was applied on the gear tooth surface as shown by the highlighted area in Figure 9. The total bending load was 180 KN (40.5 kips), uniformly distributed. Constraints were applied so that the gear would not shift or rotate under the bending load.

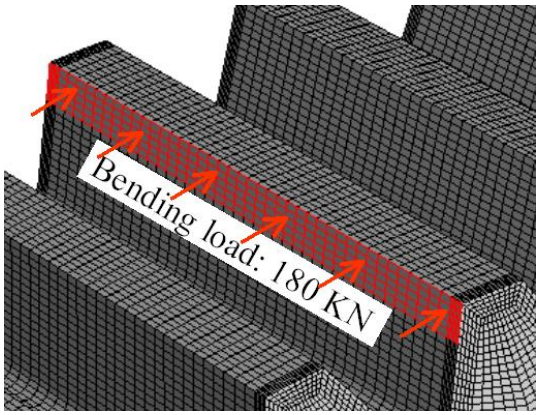

Figure 9: Schematic plot of bending load.

Figure 10 shows a comparison of the maximum principal stress change in the gear root under bending fatigue load with and without considering the residual stresses from the induction hardening process. The contour map is is a cut-view through the middle height of the gear. Both contour plots in Figure 10 share the same legend scale. By applying a bending load to the gear tooth surface, the stress in the gear root shifts from compression to tension. On the opposite tooth root, the compressive stress is enhanced. Under load, the location of the highest maximum principal stress is not in the center of the gear root. Simulations have shown that the highest stress point moves from the gear root and onto the tooth with increasing bending load.

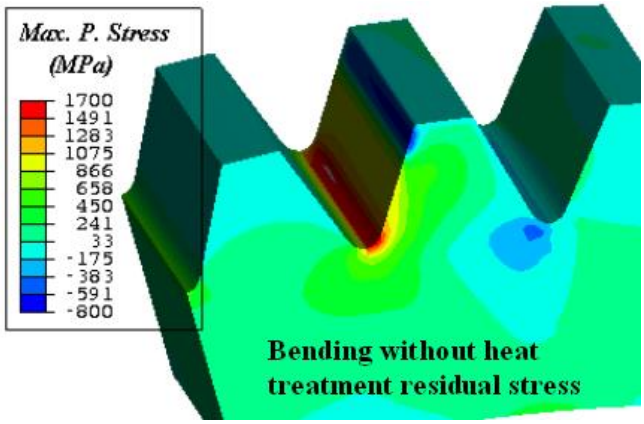

(a)

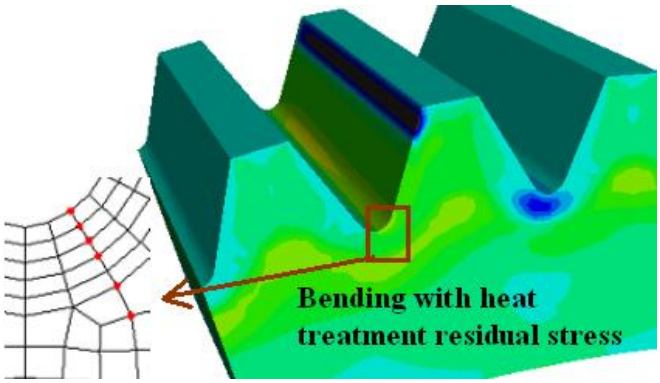

(b)

Figure 10: Comparison of maximum principal stress under fatigue bending load (a) without including the heat treatment residual stress (b) with including the heat treatment residual stress.

For a more detailed examination of the root stress due to the bending load, a line of nodes were selected in the region adjacent to the gear root, and the stress magnitude was then plotted in terms of depth. The selected nodes are shown by the magnified figure on the left side in Figure 10(b).

Figure 11 plots the maximum principal stress distiburion along this selected profile for the gear tooth under the 180 KN bending load. Without considering the heat treatment residual steress, the maximum principal stress on the gear root surface under loading is about 1650 MPa (239 ksi). However, including the effect of the compressive maximum principal stress due to the induction hardening, the predicted loading stress becomes a realistic 850 MPa (123 ksi). The difference between the predicted loading stresses is about 800 MPa (116 ksi), which is very significant. Under a 1650 MPa maximum

principal stress on the root surface, the gear would immediately fail by simple overload. However, by reducing the maximum stress to 850 MPa because of the presence of residual compression, the gear will carry the load with eventual failure likely in bending fatigue. In conclusion, the residual stress from heat treatment needs to be considered to characterize the internal stress state in the gear under bending load. Heat treatment simulation provides a practical method to assessing the material mechanics during bending fatigue stress characterization.

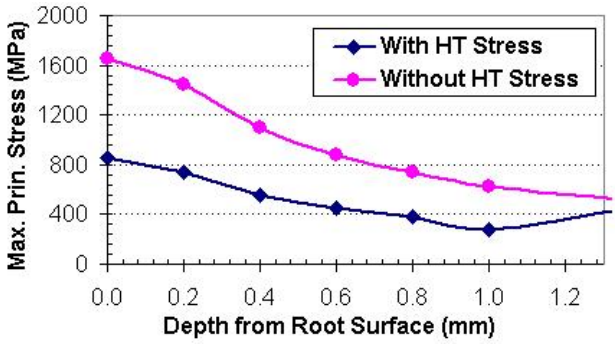

Figure 11: Line plot of maximum principal residual stress in terms of depth from root surface under fatigue bending load.

Conclusions

The induction heating process of a straight spur ring gear was modeled using DANTE. Instead of modeling the induction heating physics, the heat energy generated by the induced eddy current was used as input to drive the heating model. The spray quenching process was then optimized using sensitivity analysis. Simulation results show that both the distortion and residual stresses are sensitive to the cooling rate on the gear tooth surface, and, in this case, also the gear bore surface. For gears made of different steel grades and of different geometries, the optimum water spray processes would be different, but simulation offers a method for optimizing the individual cases.

By mapping the residual stresses from the heat treat simulation onto a whole gear model, a tooth bending model was developed to predict the root stress state. Predictions showed that residual compressive stress in the gear obtained from induction hardening process is critical to fatigue life. Heat treat processes such as induction hardening that impose significant residual compressive stress in the tooth and root surfaces act to reduce the bending stress in the tooth surface. If this residual stress is ignored, as it is in conventional AGMA gear stress calculation methods, the predicted bending stress in the gear root is exaggerated significantly. In this manner, characterizing the residual stress profile from heat treatment through simulation presents significant engineering value.

References

1. W. R. Schwenk, Simultaneous Dual-Frequency Induction Hardening, Heat Treating Progress, 35-38, (April/May 2003)
2. B. Lynn Ferguson, A. Freborg, and G. Petrus, “Software Simulates Quenching”, Advanced Materials and Processes, H31-H36, August (2000)
3. D. Shick, D. Chenoweth, Development of Carburization and Quenching Simulation Tool: Determination of Heat Transfer Boundary Conditions in Salt, Proceedings of the Second International Conference on Quenching and the Control of Distortion, 357-366, (1996)
4. Z. Li, R. Grandhi, and R. Srinivasan, Distortion Minimization during Gas Quenching Process, Journal of Materials Processing Technology, 249-257, 172(2006)
5. Z. Li, R. Grandhi, Optimal Heat Treatment Design in Manufacturing, The 7th International Conference on Numerical Methods in Industrial Forming Processes, 18-21 6(2001), Toyohashi, Japan
6. National Center for Manufacturing Sciences, “Predictive Model and Methodology for Heat Treatment Distortion: Phase 1 Summary Report”, NCMS Report 0383RE97, September 30, 1997.
7. Z. Li, B. Lynn Ferguson, and A. M. Freborg, “Data Needs for Modeling Heat Treatment of Steel Parts”, Proceedings of Materials Science & Technology Conference, 219-226, September (2004)
8. B. Lynn Ferguson, A. Freborg, Z. Li, Residual stress and Heat Treatment – Process Design for Bending Fatigue Strength Improvement of Carburized Aerospace Gears, 95-104, April (2007)